

ACOUSTIC EMISSION DURING FATIGUE OF AIRCRAFT ALUMINIUM ALLOYS

G. CLARK, P.K. SHARP and J.Q. CLAYTON

Airframes and Engines Division, DSTO Aeronautical and Maritime Research Laboratory, Melbourne.

ABSTRACT:

This paper describes a series of experiments examining the effects of loading variables on acoustic emission (AE) during fatigue of two differently processed 7050 Aluminium alloys. The experiments were intended to explore the conditions under which acoustic emission had been observed in the late stages of an AMRL fatigue test on a large stand-alone fighter aircraft bulkhead.

Investigation of the effect on AE of varying the stress ratio identified a major AE source during the loading part of the cycle under constant amplitude loading. Little or no peak-load noise was detected. The major noise source was consistent with crack face contact and/or rubbing. The use of a simple periodic-overload variable amplitude loading sequence confirmed the results of the bulkhead test, in that when crack growth occurred by stable tearing at the overloads at a very late stage in the test, high levels of peak-load AE were observed. Several mechanisms could explain this behaviour, but it is clearly associated with the rapid movement of the crack tip plastic zone through a relatively large volume of material.

Apart from the potential use of the overload-associated AE to detect fatigue cracking late in specimen life, the use of the other sources of AE identified in these tests is inherently unreliable, since most of the AE is associated with crack closure and crack load history, and was for example, extremely sensitive to the occurrence of individual overloads and underloads which could change the level of AE output dramatically and for an extended period of crack growth.

INTRODUCTION

Acoustic emission (AE), ie. detection of elastic waves originating from the growth of cracks, has long been used to detect areas in steel structures which are noisy and which therefore potentially contain defects; techniques for locating the source of acoustic noise in a loaded structure or component by triangulation are now well developed and have been extremely successful. The use of AE to detect growing fatigue cracks, in particular, is a very demanding challenge, since the crack increment per load cycle is usually very small, and the acoustic energy is released incrementally over many cycles, unlike the situation in a proof test, where higher energy release rates provide AE signals high enough to favour triangulation methods. There are many possible sources of AE, which may all be acting at the same time, making it very difficult to separate out the individual AE sources, without the use of expensive and sophisticated electronic equipment to quantify and evaluate the signal (Buttle and Scruby, 1990; McBride *et al.*, 1981). This evaluation generally takes the form of deductions based on empirical correlation between the measured signal feature and known physical anomalies.

A stand-alone bare bulkhead test, undertaken at AMRL (Anderson and Revill, 1990) was monitored using an AE system, and had shown an increase in AE output during the last 5-10% of life when the crack was of significant size. On the basis of this experience, tearing-related AE was therefore postulated as a possible explanation for the late onset of AE in the bulkhead case. Subsequent examination of the fracture surface confirmed that tearing had indeed occurred during the period when the AE output was high, and the present series of experiments was designed to investigate further this possible link, and the reliability of AE monitoring under such circumstances. Simple laboratory experiments were used, paying particular attention to the elimination of spurious noise sources, in an attempt to associate a particular AE signal with its mechanism by simple reference to the load cycle and fracture mechanics.

EXPERIMENTAL DETAILS

7050 Materials and Microstructures

Two commercial-grade aluminium alloys with differing microstructures, but each conforming to Specification 7050-T73651, were selected for investigation (Barter *et al.*, 1990). The alloys were chosen with two objectives in mind; firstly, to provide AE information about a particular microstructure used in the aircraft fleet, and secondly, by comparison, to provide information about potential variations in AE characteristics of the 7050 class of alloys as a whole.

1. The first alloy (P) was material extracted from the remnants of the FS-488 bulkhead test article referred to earlier. The microstructure retained characteristics of the cast structure and varied considerably through the plate thickness. Overall, it had a relatively coarse, duplex-grained appearance, with many coarse inter- and intra-granular inclusions.
2. The second alloy (material S, supplied as 13mm thick sheet) was representative of material subjected to a much greater level of working during manufacture, consisting of fine homogeneous grains, and a dispersion of relatively fine inclusions; it therefore represented the more heavily-worked surface regions of the thick-plate material P.

Specimens

From each material compact tension specimens (CTS) (see Fig.1) were machined in close accordance with ASTM E647, with a thickness of 12.7mm and an initial starter notch at an a/W ratio of 0.375 (where a is the crack length and W the specimen width). The specimen geometry varied from ASTM E647 by having a small circular region machined on the back face to facilitate correct placement of the AE probe, and several small holes in the front face to accommodate screw attachments for potential drop crack length measurement. The specimen surface was polished to allow optical crack length measurement.

Mechanical Tests and AE Set-up

Cyclic loading tests were carried out on a 50 kN servo-hydraulic testing machine. Particular attention was given to methods for attenuating spurious noise which would confuse the results. Specially-designed grips (Martin, 1984) were used to attenuate background AE noise transmitted to the specimen via the loading frame. Preliminary tests with and without a hydraulic supply confirmed that the grip setup attenuated hydraulic noise to a level below the background (static) level. However, significant pin noise was still observed during the bottom 15% of the load curve; this was present from the commencement of the test. The noise was confirmed as coming from the pins by testing a keyhole sample (ie. a specimen identical except that it had a rounded notch which would produce no crack-related or high-strain AE) at the same fatigue loads.

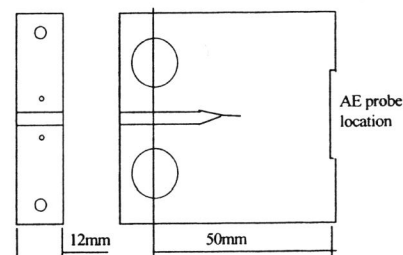


Figure 1. CTS Test specimen dimensions, $a/W = 0.375$. The machined hole at the back of the specimen locates the AE probe.

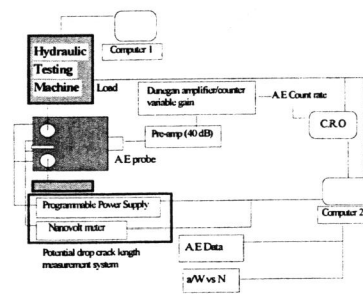


Figure 2. AE system used during the test program. Computer 1 controls the hydraulic test machine while computer 2 does all the data acquisition and data processing

The AE setup involved a Dunegan/Endevco 9203A resonant probe (sensitivity 60.7 dB below $V/m/s$), fixed gain preamplifier and Dunegan/Endevco 302A/303 Amplifier-Counter. The AE signal, processed to give the count rate (or time-derivative), and the load cell signal were fed into a storage CRO so that signals could be inspected. The signals were also digitised and captured by computer, to be processed later. The digitising rate, sampling period and amplifier gain were the principal variables used in the experiments. The AE experimental set-up is shown schematically in Figure 2.

Testing Method.

Constant-amplitude and varying R-ratio tests

The first tests were run using fairly simple conditions in order to examine basic features of the AE output; a relatively constant P_{max} (maximum stress) with two different stress ratios $R (=P_{min}/P_{max}) = 0.1$ and $R = 0.5$. The fatigue crack in the sample was grown at 5 Hz ($R=0.1$) for 0.5 to 0.7 mm, before the test was then slowed to 1 Hz and AE collected over numerous cycles. The stress ratio was then increased to $R = 0.5$ and AE again collected. In both cases the specimen was allowed a few cycles to settle in at its new frequency or stress ratio before AE was recorded. The stress ratio was adjusted back to $R = 0.1$ and the fatigue crack continued until the whole process could be repeated at another crack length. This allowed data to be collected for materials P and S at the two different R values for similar crack lengths and loads.

The test was set up to collect all the AE coming from the specimen over a wide range of frequencies, with no effort being made to locate the source directly. In this way it was hoped that AE sources could be identified by reference to the loading variables, though care was taken to ensure that any external noise would be detected and identified.

Periodic overload tests

In these tests, the fatigue crack was grown in specimens manufactured from bulkhead material III under approximately constant load amplitude conditions, with an overload to 130% inserted every 10000 cycles. The crack was allowed to grow, thus increasing the stress intensity until, it was hoped, stable tearing would occur, simulating the conditions experienced in the bulkhead. The AE was monitored for 5 seconds before and after each overload, all at 1Hz.

RESULTS

Microscopy

Analysis and comparison of the two microstructures has been reported elsewhere (Barter *et al.*, 1990). While both materials are 7050-T7451, the different microstructure of the two samples had a significant effect on the fracture surface. The bulkhead material P (with its coarser microstructure) had a very rough fracture surface, with large surface asperities and extensive black oxide produced by rubbing. The fracture surface of material S, however, from the heavily-worked plate, was quite smooth in comparison and while signs of rubbing were present, it had not occurred to the extent of that seen in the thick-plate material.

AE from Constant Amplitude Fatigue

The favoured means of presenting the results is through superposition of the AE detected (shown as count rate) on the load cycle, to aid identification of the source. Figure 3 presents typical results material S; for three different crack lengths, several load cycles are shown. The AE observed on the low part of the falling-load side of the cycle was associated with the loading system.

Rising-load AE

Both materials showed evidence of AE on the rising-load part of the cycle (as shown in the examples in Figs.3, 4, 5 and 6). In some cases, the noise occurred at the low-load/medium-load

part of the cycle, while in others, a second occurrence of AE was present at higher loads. Sometimes the two blended together, but there were sufficient examples of the two appearing as separate peaks to suggest that two distinct mechanisms were involved. Two mechanisms seem capable of operating at these loads; one is AE from crack face "unsticking" i.e. the release of elastic energy when substantial load transfer between faces effectively ceases. The other, more likely associated with AE which occurs elsewhere on the rising-load part of the cycle (in some cases up to 80% of peak load), is rubbing between individual asperities, either through natural surface topography or assisted by a microscopic mode II crack tip displacement component. The two modes (unsticking and rubbing) are described collectively here as rubbing. The rubbing AE increased with crack length as shown in Fig.3.

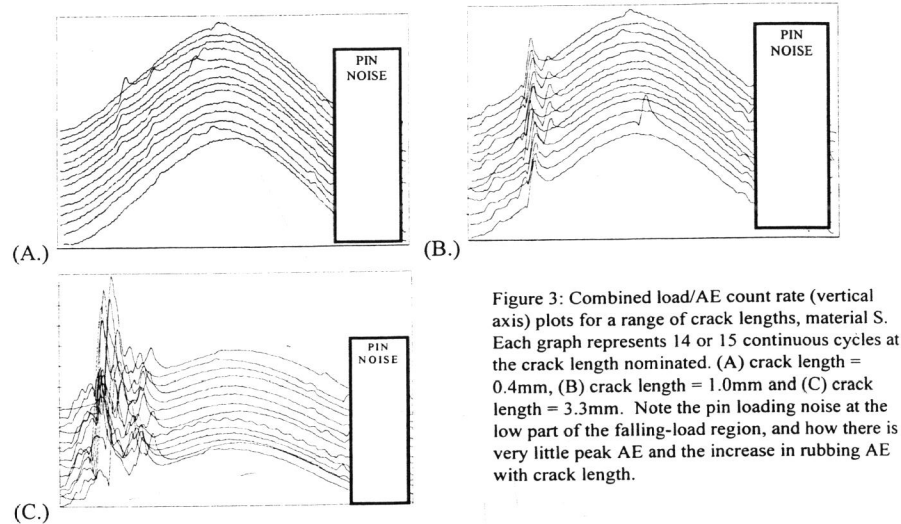


Figure 3: Combined load/AE count rate (vertical axis) plots for a range of crack lengths, material S. Each graph represents 14 or 15 continuous cycles at the crack length nominated. (A) crack length = 0.4mm, (B) crack length = 1.0mm and (C) crack length = 3.3mm. Note the pin loading noise at the low part of the falling-load region, and how there is very little peak AE and the increase in rubbing AE with crack length.

The two materials behaved differently, as shown in Figs. 3 and 5; the rubbing noise from the rough-surface thick-plate sample extended up to 80% of the peak cyclic load, whereas the smooth-surface thin-plate sample produced AE only up to 50% of peak cyclic load, and usually in smaller amounts, again consistent with crack face contact mechanisms.

Peak-load AE

Little peak-load AE was observed in both materials.

Falling-load AE

There is evidence in Fig.3 of small amounts of AE on the falling-load side of the load cycle, separate from the pin noise identified earlier. This AE was intermittent, and at a fairly low level. Its occurrence on the falling part of the cycle is consistent with it coming from contact or rubbing between the crack faces on the closure part of the cycle.

Effect of mean stress

Figure 4 compares AE from material S for similar crack lengths at $R = 0.1$ and $R = 0.5$. No distinct or consistent AE was detected at the higher mean stress.

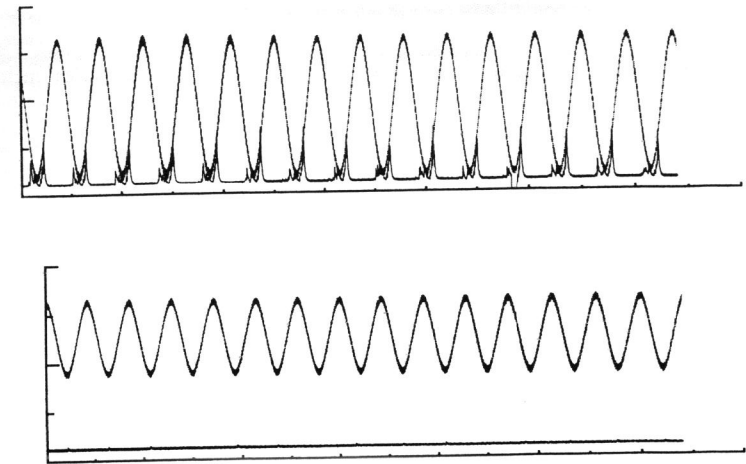


Figure 4. Graph of the effect of R ratio on AE. The horizontal axis is time showing a number of consecutive cycles and the vertical axis is load or AE counts. Material S, 13mm plate at $R=0.1$, (top) and $R=0.5$ (bottom). Note the decrease in AE at the higher R value.

Addition of oil

For both materials the addition of oil into the fatigue crack produced a significant reduction in AE from crack face rubbing (illustrated for material P in Fig.5) to the point that in many cases no AE was detected at all anywhere on the load cycle.

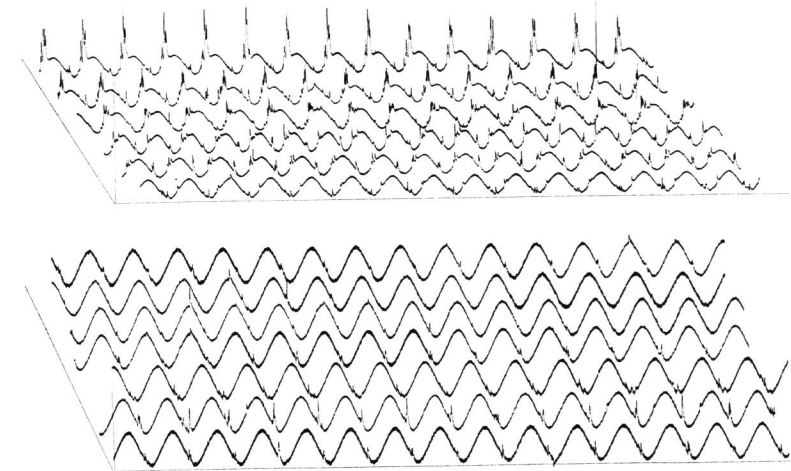


Figure 5. Graph of the effect of oil on AE. The horizontal axis is time showing a number of consecutive cycles and the vertical axis is load/AE counts. Material P at $R=0.1$, (left) without oil (right) with oil. Note that there is more rubbing AE than for the S material, and that oil addition reduced rubbing noise. The pin noise, however, remains.

AE from Variable-Amplitude Fatigue

Figure 6 shows examples of the combined load/AE output signal sampled at various stages as the crack grew through the specimen. Each row represents a series of load cycles, including one overload.

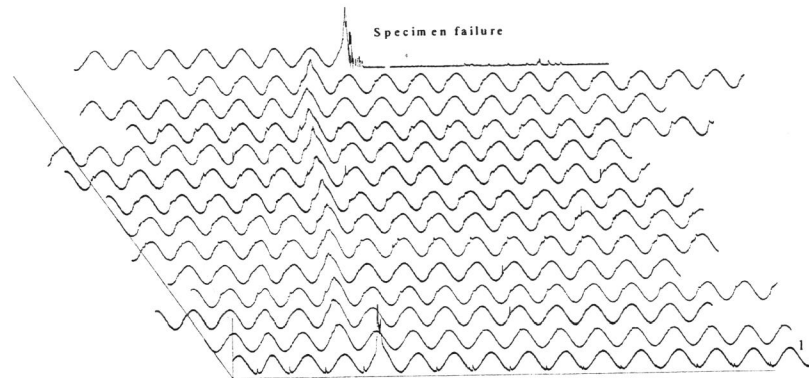


Figure 6. Combined AE count rate/AE data for the variable-amplitude loading tests. Each row of cycles shows the 130% overload (obvious because of the increased AE), and neighbouring cycles of baseline loading. Crack length increases from front to back, with failure occurring on the last overload cycle shown.

The baseline-cycling peak load AE remained at a very low level (much lower than the rubbing noise, and invisible in Fig. 6) throughout the majority of crack growth. However, the AE which occurred during overload was a dominant feature; it was high during the initial overload in the test, and then decreased to a fairly steady condition, before rising in the last few overloads of the test. Subsequent examination of the fracture surfaces confirmed that stable tearing was visible on the surface, associated with the last few overloads.

Rubbing AE was very low at short crack lengths, so that the overload AE dominated. As the crack extended, the rubbing increased, as had been observed in the earlier tests. Interestingly, however, at very long crack lengths, the rubbing AE decreased slightly.

DISCUSSION

Constant-Amplitude tests

The results suggest that the majority of the AE observed emanates from rubbing of the crack faces. The rubbing-sourced AE could be made to disappear by varying the loading conditions, and by introducing an oil environment, confirming the nature of the source as crack face contact and rubbing.

The rougher fracture surface of material P provided the greatest amount of AE in the rising load part of the cycle, and this is attributed to increased rubbing of crack face asperities, and the AE noise on the rougher fracture surface occurred over a wider load range, again, consistent with a roughness-induced AE source. As would be expected, at the high stress ratio $R=0.5$, the rubbing AE disappeared in both materials.

Figure 7 shows schematically the different parts of the load cycle in which AE was detected, and indicates the most likely source mechanism. The identification of individual AE signals on the rising load side of the cycle as "unsticking" or rubbing mechanisms is difficult, since both AE

signals tended to disappear and reappear in a cyclic manner, consistent with changes in crack face morphology. The "unsticking" process could be simply be the fracture of mechanically-keyed asperities at a well-defined (usually low) load. Rubbing, in contrast, as observed, would be expected to occur over a range of loads, and to vary with time and crack length. Occasional AE spikes were picked up at or near peak load, but these tended to be relatively small compared to the rubbing spikes and in the majority of cycles the peak load was noiseless. What signal was present would be expected to be associated with fracture processes in the high strain crack tip process zone, or fracture of inclusions.

The falling-load AE was similar to that on the rising-load side, but with much lower amplitude and count rate. In many cases, distinct AE was observed repeatedly at a single well-defined load level, possibly associated with crack face contact, but rubbing would also be expected to occur at loads near this contact load; it is difficult to identify AE signals positively with either mechanism.

A major conclusion from these results is that while the AE can be identified with specific mechanisms and processes occurring during fatigue, the major AE type in these alloys is exceptionally sensitive to changes in loading history which affect crack closure and crack face rubbing. As a means of tracking fatigue crack growth, AE is therefore inherently unreliable in these alloys.

Overload tests

The introduction of overloads into the test sequence led to generation of peak-load AE on each overload. Some of the "overload" AE, with fairly low amplitude, was observed throughout the test, and presumably arises from the rapid growth of the crack tip plastic zone and process zone causing a burst of inclusion fractures or other rapid events. Late in the test, however, the onset of more rapid crack advance through stable tearing appeared to be accompanied by increased "overload" AE. The tearing necessarily introduce rapid growth of the plastic zone, rapid movement of the crack tip plastic zone and process zones though a large volume of material, and extension of the crack into new material, and hence would be expected to promote rapid operation of all of the mechanisms normally operating in crack extension, and possibly others. Examples of possible AE sources include inclusion fracture and rapid unloading of ligaments. The observation of high levels of "overload" AE were consistent with the results observed on the stand-alone bulkhead.

Rubbing AE increased throughout the test, until the crack was close to failure; at this stage, the rubbing AE appeared to decrease slightly. This is consistent with the higher crack growth rates in this regime, in that higher growth rates will decrease the ability of asperities to make contact through rubbing.

General

Overall, the different types of AE observed throughout these tests displayed two different types of variability. One was a cycle-to-cycle variation in output, and the other was a much longer-term drift in amplitude (over perhaps hundreds or thousands of cycles). The high level of AE associated with crack opening and rubbing would explain these variations, firstly, as rubbing is controlled by individual asperities on the fracture surface, which will vary as the crack front moves through, and secondly, as a result of AE being associated with rubbing which is influenced by fretting product; the accumulation and dispersal of such product could explain the longer-term variations in AE. It was clear that AE was sensitive to load history, in that anything which caused changes in crack opening (eg. an overload, or an environmental change) could lead to changes in AE in the following cycles. Unfortunately, this sensitivity to individual load cycles, and hence to load sequence makes the AE observed inherently unreliable as a means of tracking crack extension in parts experiencing complex or unknown load histories.

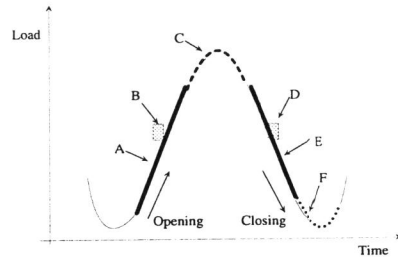


Figure 7. Schematic of load cycle and regions of AE suggested by these experiments. Regions labelled "A" and "E" arise from crack face rubbing, region "C" is the peak load noise due to plasticity, inclusion fracture and/or tearing, while regions "B" and "D" are the unsticking and crack face contact points. Region "F" is the pin noise.

CONCLUSIONS

- 1) The use of noise-minimisation techniques allowed AE to be identified with specific parts of the load cycle, and hence the mechanisms capable of generating AE.
- 2) The direct observation of crack growth by means of a reliable peak load AE output, was not possible in this 7050 Al alloy under constant- K_{max} cycling.
- 3) In contrast, AE associated with crack face rubbing and/or crack opening was easily detected on the rising-load part of the cycle, and to a much lesser extent, AE from crack closure and/or rubbing on the falling-load side. This rubbing AE generally far exceeded any peak-load AE that occurs under constant-amplitude loading conditions. The rubbing AE increases in amplitude and range over the load cycle with increasing crack length, probably as a result of a gradual build-up of fretting product in the crack.
- 4) Rubbing AE decreased with increasing the stress ratio, hence reducing crack closure, or by changing the environment, or by changing the material microstructure. In view of the highly favourable conditions maintained in these experiments, and the difficulties which would be posed by complex load and environment variations in most practical applications, the monitoring of fatigue crack growth using AE seems to be highly unreliable at present.
- 5) The occurrence of stable tearing on the fracture surface, appeared to be associated with enhancement of the peak load AE output in individual overload cycles shortly before failure. This observation reproduces those made in a stand-alone bulkhead test, and confirms that the enhancement of crack growth which occurs when stable tearing begins can be associated with enhanced AE output, allowing the possibility of crack detection before failure under limited, specific conditions of laboratory testing.

REFERENCES

- Anderson, I and Reville, G. (1990) F/A-18 Fuselage Station 488 Free-Standing Bulkhead Fatigue Test, ARL-STRUC-TM-575
- Barter, S.A., Athinotiis, N. and Lambrianidis, L. (1990) Examination of the Microstructure of 7050 Aluminium Alloy Samples, ARL-MAT-TM-403
- Buttle, D.J. and Scruby C.B. (1990) Characterisation of Fatigue of Aluminium Alloys by Acoustic Emission, Part 1 - Identification of Source Mechanism, *Journal of Acoustic Emission*, Vol 9, No. 4
- Clark, G and Knott, J.F. (1977) Acoustic Emission and Ductile Crack Growth in Pressure-Vessel Steels, *Metals Science*, 11, 531-537
- Clark, G. and Knott J.F. (1981) Acoustic emissions associated with fracture processes in structural steels. *Metals Science*, Vol 15, Nov-Dec, 481-491
- Cousland S. McK and Scala C.M. (1981) Acoustic Emission and Microstructure in Aluminium Alloy 7057 and 7050. *Metals Science*, Vol 15, Nov-Dec, 609-614
- Martin, G. G. (1984) *Acoustic Emission from 4030 Steel During Fatigue*, Ph. D Thesis, Department of Materials Engineering, Monash University, Australia
- McBride, S.L., MacLachlan, J.W. and Paradis, B.P. (1981) Acoustic Emission and Inclusion Fracture in 7075 Aluminium Alloys, *Journal of Non-Destructive Evaluation*, Vol 2, No.1